Supplement of Atmos. Chem. Phys., 18, 6187–6206, 2018
https://doi.org/10.5194/acp-18-6187-2018-supplement

Atmospheric Chemistry and Physics
Open Access
EGU

Supplement of

Advanced source apportionment of carbonaceous aerosols by coupling offline AMS and radiocarbon size-segregated measurements over a nearly 2-year period

Athanasia Vlachou et al.

Correspondence to: André S. H. Prévôt (andre.prevot@psi.ch) and Imad El Haddad (imad.el-haddad@psi.ch)

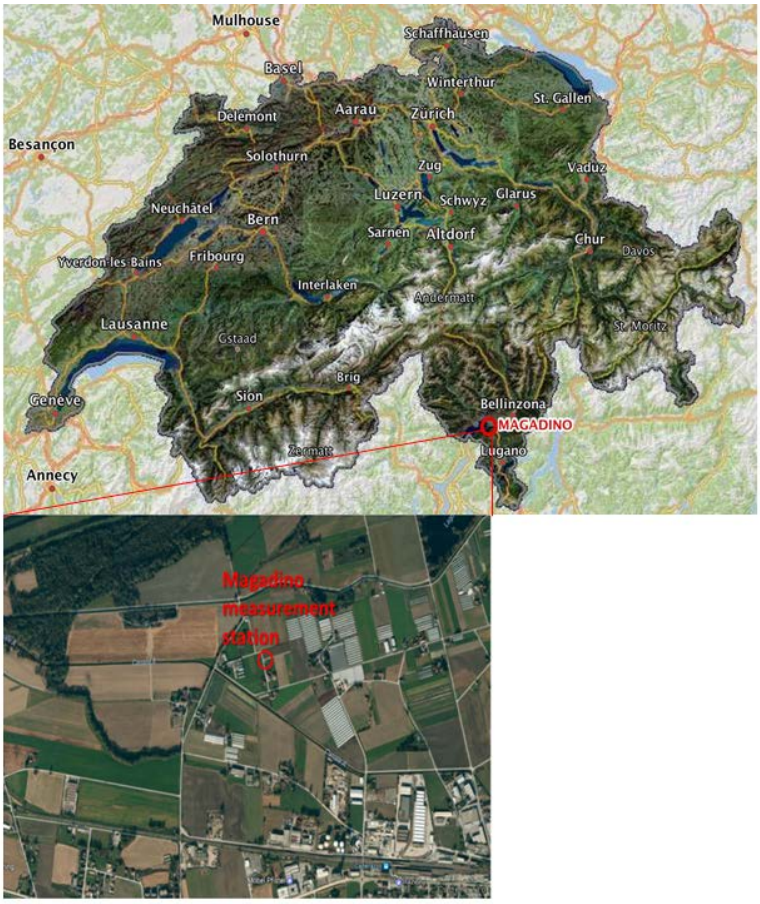

Figure S1. Sampling location.

S.1 Exploration of PMF solutions

To understand the variability of our dataset we explored several constrained PMF solutions with a total of 4-10 factors. With a four-factor solution, a biomass burning OA (BBOA) factor was resolved exhibiting a high contribution of the fragment $C_2H_4O_2^+$, a typical marker for BBOA which originates from the pyrolysis of cellulose. In addition, this factor was significantly enhanced during winter which is expected due to the increased residential wood burning activity during this time of year in Magadino. However, the BBOA factor included some sulphur-containing fragments which are not expected in such a profile. Daellenbach et al. (2017) resolved for the first time a sulphur-containing factor (SCOA) with a similar off-line AMS analysis in their study about long-term chemical analysis of OA at 9 sites in Switzerland and Liechtenstein, including Magadino. In our case it seemed that SCOA was mixing with BBOA in this 4-factor solution. The other two factors included an oxygenated OA (OOA) with high contribution of the fragment CO_2^+, but with no distinct yearly cycle and a factor with notable *m/z* 43 ($C_2H_3O^+$) and *m/z* 61 ($C_2H_5O_2^+$) signals enhanced in summer which seemed to be a mixing between a primary and a secondary OA factor. Bozzetti et al. (2016) were the first to identify a primary biological OA (PBOA) factor whose mass spectrum resembled the mass spectra of plant debris and biological carbohydrates, with fragments like $C_2H_4O_2^+$ and $C_2H_5O_2^+$ being particularly enhanced. Such a factor is also expected at our measurement site, therefore we checked if a solution with a higher number of factors could lead to such a separation.

A five-factor solution resulted in a reduction of the residuals and a clearer separation of the BBOA. However, PBOA and SCOA were still not clearly separated. A six-factor solution allowed for a segregation of the OOA into two different factors, with one showing increased concentrations during winter. Moreover, the SCOA could be better isolated, describing the variability of the $CH_3SO_2^+$ fragment and was dominant for the coarse ($PM_{2.5\text{-}10}$) size fraction.

Yet, the PBOA factor was clearly identified with the introduction of a seventh factor which exhibited a distinct enhancement in the coarse fraction in spring and summer. This seven-factor solution resulted in a further decrease of the residuals and the resolution of three oxygenated factors. Two of which were named after their seasonal behaviour, winter and summer OOA (WOOA and SOOA), as proposed by Daellenbach et al. (2017). The third OOA exhibited a rather stable yearly cycle and high contribution at *m/z* 44 (CO_2^+); see below in Fig. S5. As this factor was mainly fossil and correlated with fossil OC (as explained in Section 4.3 of the main text), we called this factor anthropogenic OOA (AOOA). However, note that AOOA was not the only anthropogenic OOA factor; WOOA was also related to non-fossil anthropogenic activities such as wood burning (see Section 4 of main text). Higher order solutions resulted in a further splitting of the oxygenated factors WOOA and AOOA, which could not be interpreted. Hence, we selected this seven-factor solution.

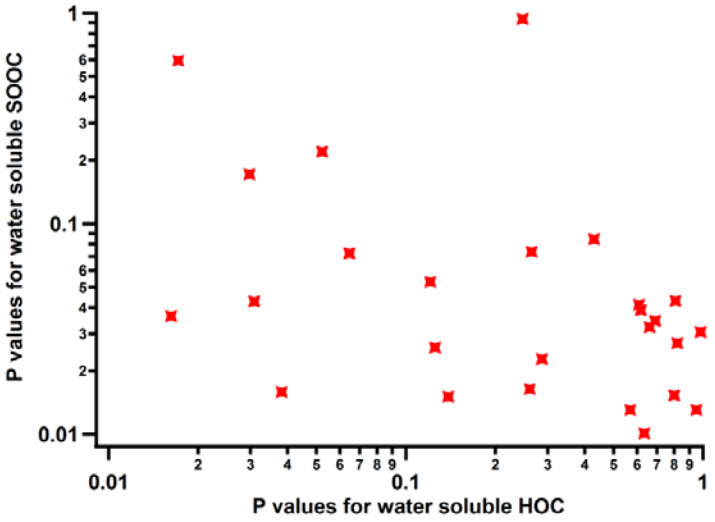

Figure S2. Scatter plot with p-values from the comparison of the two size fractions for the selected solutions of the water soluble factors SOOC and HOC (WSSOOC and WSHOC) (see main text Section 3.3 for conversion of WSOA to WSOC). Some data points from the factors WSSOOC and WSHOC exhibited higher concentrations for the $PM_{2.5}$ size fraction compared to PM_{10}, which is not physically possible as aerosols collected by a PM_{10} inlet include also the $PM_{2.5}$ size fraction.

Table S1. P-value range resulting from the correlation between a water soluble factor in PM_{10} and the respective one in $PM_{2.5}$.

P value range	WSHOA	WSBBOA	WSPBOA	WSSCOA	WSAOOA	WSSOOA	WSWOOA
Min	1.08E-05	4.00E-04	1.04E-06	1.30E-13	6.86E-10	8.02E-08	7.66E-3
Max	0.99	0.33	0.01	0.77	0.33	0.94	0.99

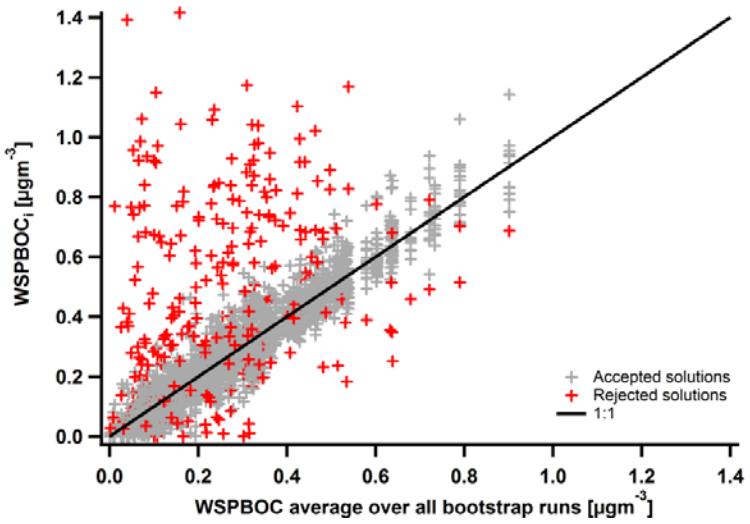

Figure S3. Example of a scatter plot between each bootstrap solution i and their average for the water soluble PBOC (WSPBOC) factor.

S.2 Recoveries weighting factor

To select the physically meaningful recoveries we applied a weighting factor f calculated by the following equation:

$$f = \begin{cases} 1 & ,for\ 0 < R_{i,k,max} \leq 1 \\ \dfrac{\frac{1}{\sigma\sqrt{2\pi}} exp * \left(-\frac{\left(R_{i,k,max} - \mu\right)^2}{2\sigma^2} \right)}{\frac{1}{\sigma\sqrt{2\pi}} exp * \left(-\frac{(1-\mu)^2}{2\sigma^2} \right)} & ,for\ R_{i,k,max} > 1 \end{cases} \quad \text{(S1)}$$

Where σ = 0.05, μ = 1, i the number of iterations and k the factor.

A visualisation of the weighting factor is shown in Figure S4.

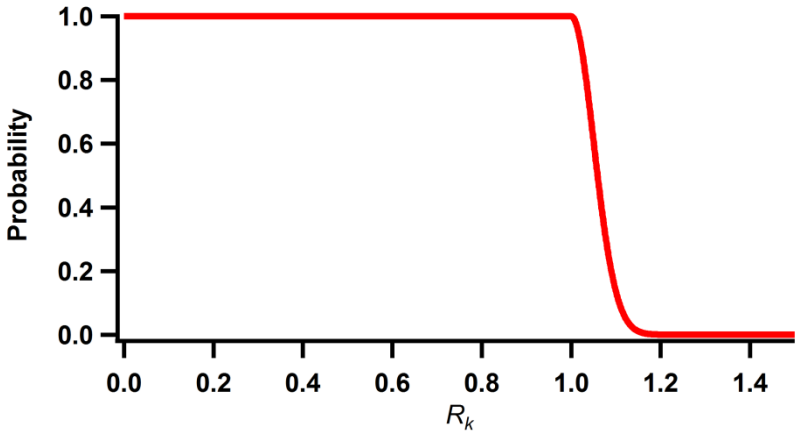

Figure S4. Probability of R_k occurrence: all R_k that exhibited values between [0,1] are weighted by 1 and the R_k > 1 are downweighted. Even though R_k > 1 is physically not plausible errors in OC and WSOC may allow such values.

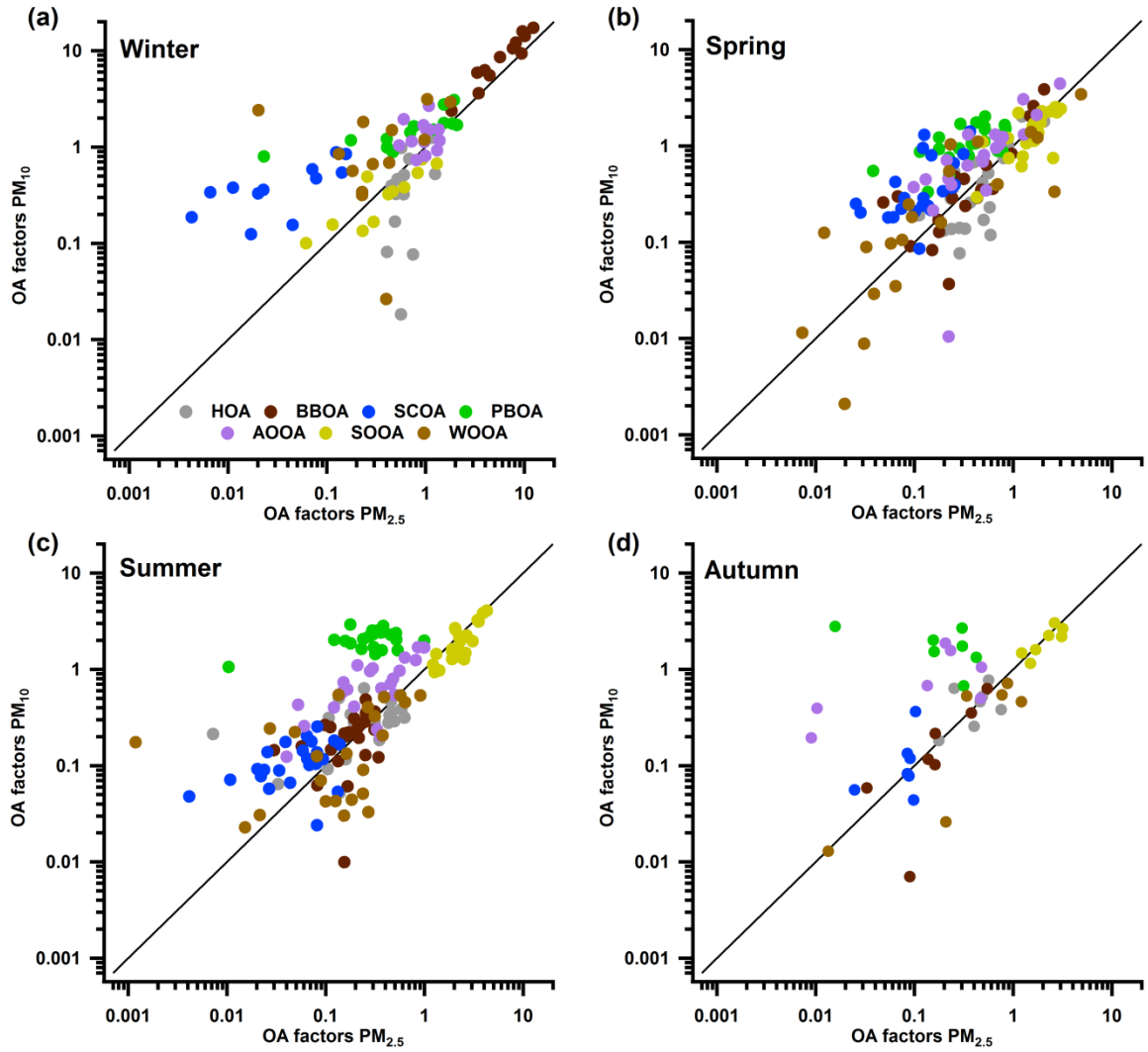

Figure S5. Scatter plots between OA factors in PM_{10} and $PM_{2.5}$ for winter (a), spring (b), summer (c) and autumn (d).

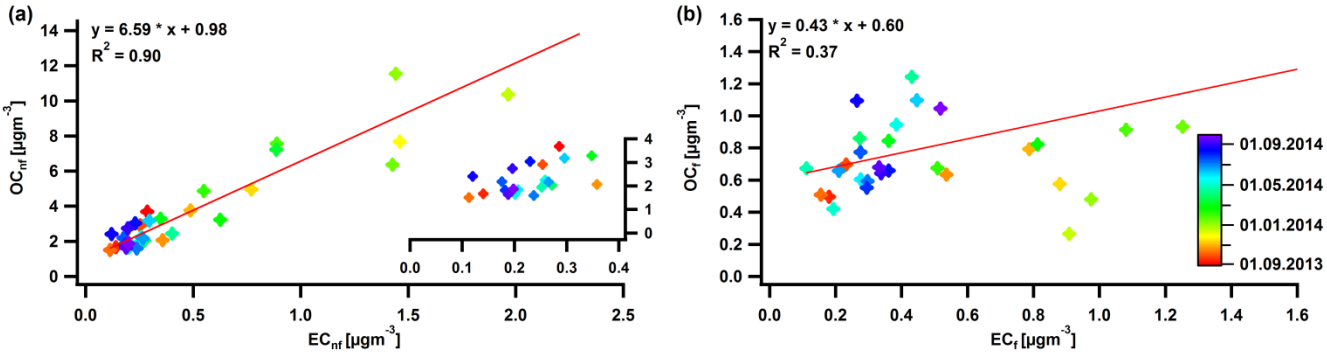

Figure S6. Correlation between OC_{nf} and EC_{nf} with a zoom at the points in summer, late spring and early autumn (a) and correlation between OC_f and EC_f (b). The R^2 for the selected data points in the zoomed plot is 0.29.

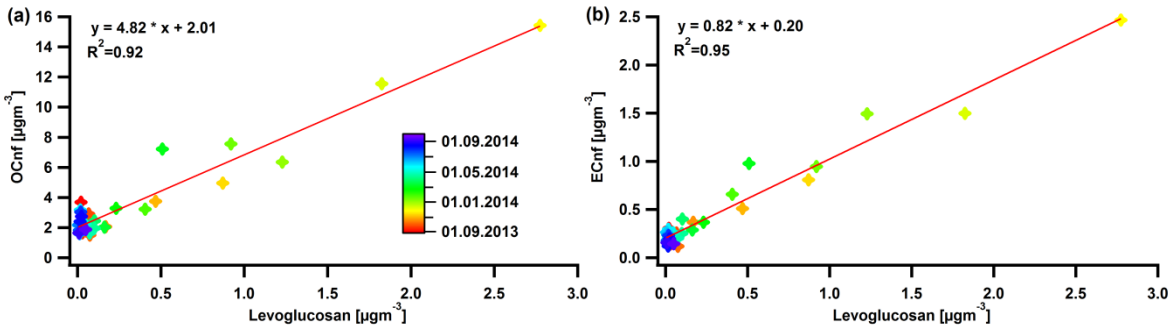

Figure S7. Correlations between OC_{nf} (a) and EC_{nf} (b) with levoglucosan.

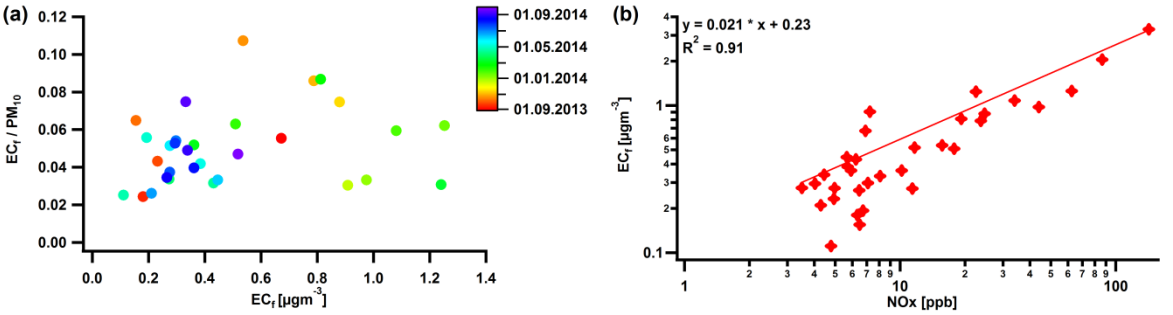

Figure S8. Correlations between:
(a) the ratio EC_f /PM_{10} and EC_f. The fact that the ratio EC_f /PM_{10} remains constant with the increase of EC_f indicates that the EC_f variability is influenced by meteorology.
(b) EC_f and NOx. Note that the regression line shows a linear relationship.

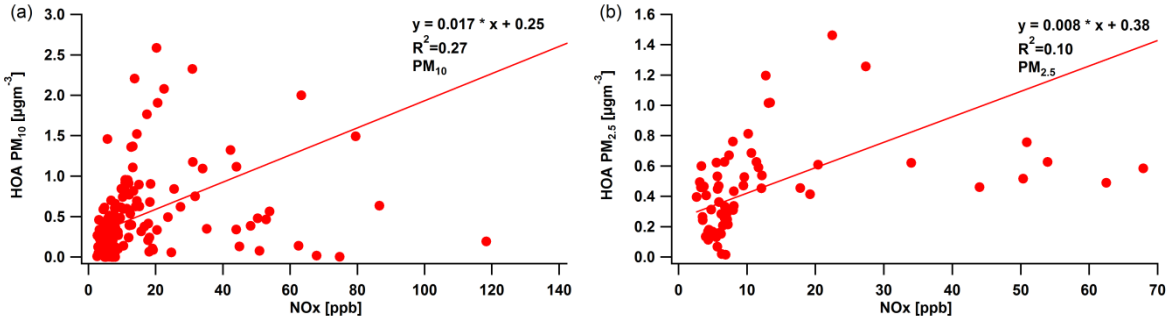

Figure S9. Scatter plot between HOA and NOx for PM_{10} (a) and $PM_{2.5}$ (b).

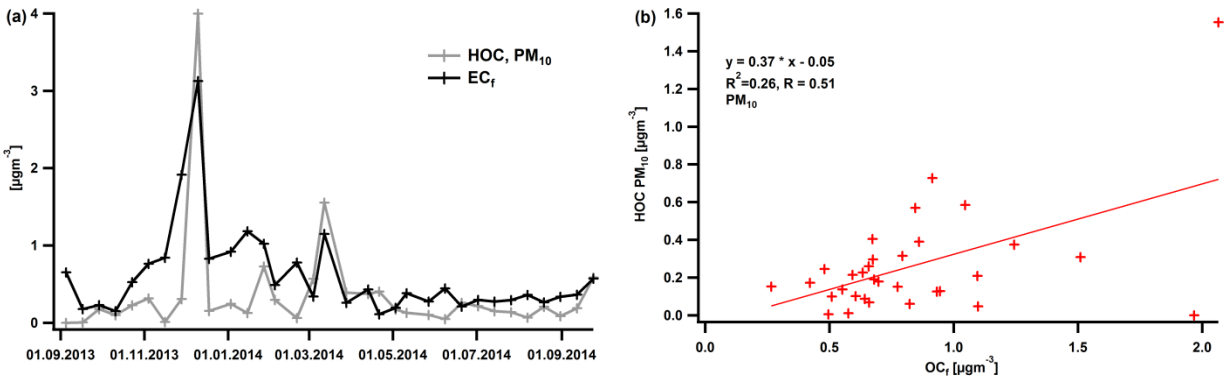

Figure S10. Time series of HOC and EC_f (PM_{10}) (a) and scatter plot between HOC and OC_f (b).

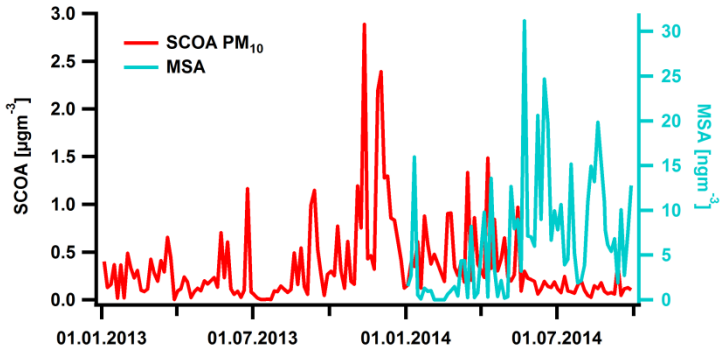

Figure S11. Time series of SCOA and MSA for PM_{10}.

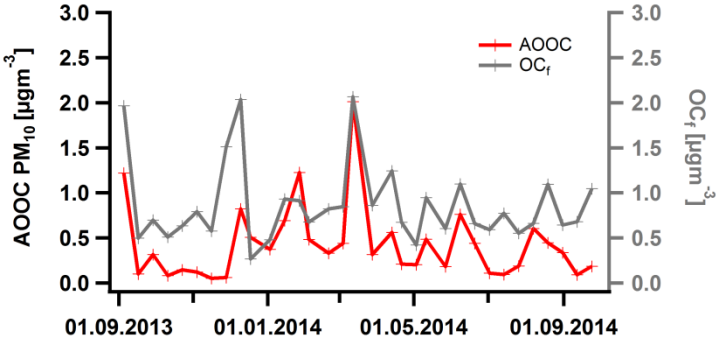

Figure S12. Timeseries of AOOC and OC_f.

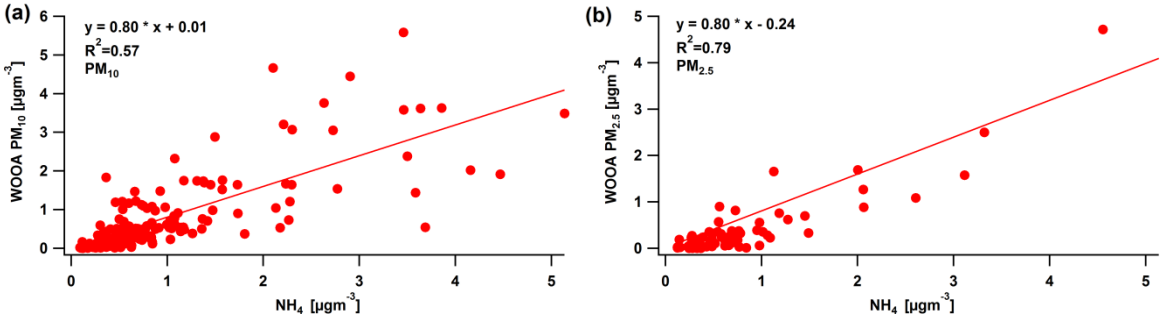

Figure S13. Correlations between WOOA and NH_4^+ for PM_{10} (a) and $PM_{2.5}$ (b).

Table S2. Season-wise averaged concentrations (± one standard deviation) for all OC factors separated for the two size fractions where available.

	Autumn			Winter			Spring			Summer		
μgm^{-3}	2013 (Sept, Oct, Nov)	2014 (Sept)		2013 (Jan, Feb, Dec)	2014 (Jan, Feb)		2013 (Mar, Apr, May)	2014 (Mar, Apr, May)		2013 (Jun, Jul, Aug)	2014 (Jun, Jul, Aug)	
	PM10	PM10	PM2.5	PM10	PM10	PM2.5	PM10	PM10	PM2.5	PM10	PM10	PM2.5
HOC	0.17±0.15	0.35±0.16	0.33±0.14	1.04±1.02	0.34±0.27	0.49±0.19	0.51±0.42	0.39±0.40	0.40±0.34	0.09±0.10	0.21±0.11	0.19±0.14
BBOC	1.75±2.14	0.12±0.12	0.12±0.10	4.70±3.15	5.36±2.64	3.83±1.81	0.77±0.68	0.38±0.54	0.28±0.31	0.08±0.06	0.12±0.06	0.11±0.05
$SCOC_f$	0.28±0.32	0.06±0.05	0.04±0.01	0.22±0.26	0.21±0.13	0.03±0.03	0.10±0.08	0.21±0.17	0.07±0.04	0.08±0.12	0.05±0.03	0.03±0.02
$SCOC_{nf}$	0.06±0.07	0.01±0.01	0.01±0.003	0.05±0.06	0.05±0.03	0.01±0.01	0.02±0.02	0.05±0.04	0.02±0.01	0.02±0.03	0.01±0.01	0.01±0.004
PBOC	1.02±0.49	0.89±0.34	0.12±0.07	0.33±0.28	0.80±0.34	0.50±0.36	0.51±0.30	0.55±0.22	0.19±0.12	0.81±0.30	0.98±0.24	0.15±0.10
$AOOC_f$	0.28±0.24	0.32±0.22	0.08±0.07	0.46±0.24	0.49±0.19	0.35±0.10	0.49±0.24	0.38±0.35	0.23±0.23	0.50±0.23	0.27±0.16	0.13±0.09
$AOOC_{nf}$	0.08±0.07	0.10±0.07	0.03±0.02	0.14±0.07	0.15±0.06	0.11±0.03	0.15±0.07	0.11±0.11	0.07±0.07	0.15±0.07	0.08±0.05	0.04±0.03
$SOOC_f$	0.14±0.14	0.25±0.09	0.27±0.09	0.04±0.03	0.04±0.03	0.06±0.04	0.13±0.10	0.18±0.09	0.19±0.09	0.30±0.13	0.24±0.11	0.29±0.10
$SOOC_{nf}$	0.55±0.54	0.95±0.34	1.04±0.36	0.14±0.10	0.15±0.11	0.22±0.15	0.50±0.37	0.68±0.33	0.75±0.35	1.15±0.50	0.93±0.41	1.12±0.40
$WOOC_f$	0.09±0.08	0.05±0.04	0.07±0.06	0.27±0.23	0.16±0.13	0.07±0.06	0.13±0.12	0.07±0.11	0.08±0.15	0.08±0.06	0.03±0.02	0.03±0.03
$WOOC_{nf}$	0.28±0.28	0.15±0.13	0.21±0.21	0.88±0.74	0.53±0.43	0.22±0.19	0.44±0.39	0.22±0.35	0.25±0.49	0.25±0.21	0.09±0.08	0.10±0.09

References

Bozzetti, C., Daellenbach, K., R., Hueglin, C., Fermo, P., Sciare, J., Kasper-Giebl, A., Mazar, Y., Abbaszade, G., El Kazzi, M., Gonzalez, R., Shuster Meiseles, T., Flasch, M., Wolf, R., Křepelová, A., Canonaco, F., Schnelle-Kreis, J., Slowik, J. G., Zimmermann, R., Rudich, Y., Baltensperger, U., El Haddad, I., and Prévôt, A. S. H.: Size-resolved identification, characterization, and quantification of primary biological organic aerosol at a European rural site, Environ. Sci. Technol., 50, 3425-3434, doi:10.1021/acs.est.5b05960, 2016.

Daellenbach K. R., Stefenelli G., Bozzetti C., Vlachou A., Fermo P., Gonzalez R., Piazzalunga A., Colombi C., Canonaco F., Kasper-Giebl A., Jaffrezo J.-L., Bianchi F., Slowik J. G., Baltensperger U., El-Haddad I., and Prévôt A. S. H.: Long-term chemical analysis and organic aerosol source apportionment at 9 sites in Central Europe: Source identification and uncertainty assessment, Atmos. Chem. Phys., 17, 13265-13282, doi:10.5194/acp-2017-124, 2017.